European Journal of Medicinal Chemistry 44 (2009) 4681–4689

Contents lists available at ScienceDirect

European Journal of Medicinal Chemistry

journal homepage: http://www.elsevier.com/locate/ejmech

Original article

Synthesis, Raman, FT-IR, NMR spectroscopic characterization, antimicrobial activity, cytotoxicity and DNA binding of new mixed aza-oxo-thia macrocyclic compounds

Naz M. Aghatabay [a,*], A. Baş [b], A. Kircali [b], G. Şen [c], M.B. Yazicioğlu [c], F. Gücin [c], B. Dülger [d]

[a] Department of Chemistry, Fatih University, Büyükçekmece, Istanbul 34500, Turkey
[b] Department of Chemistry, Koc University, Sariyer, 34450 Istanbul, Turkey
[c] Department of Biology, Fatih University, Büyükçekmece, Istanbul 34500, Turkey
[d] Department of Biology, Canakkale Onsekiz Mart University, Canakkale, Turkey

ARTICLE INFO

Article history:
Received 24 July 2008
Received in revised form
2 June 2009
Accepted 9 July 2009
Available online 16 July 2009

Keywords:
Apoptotic
CT-DNA
Cytotoxic
FT-Raman
Inhibitory
Macrocyclic
Yeast cultures

ABSTRACT

Series of new mixed aza-oxo-thia macrocyclic ligands 1,9(2,6)-ditriazina-2,8,10,16-tetraaza-3,7,11,15-tetraoxo-5,13-dithia-cyclohexadecaphan-1^4,9^4-diphenyl (**L_1**); 1,10(2,6)-ditri azina-2,9,11,18-tetraaza-3,8,12,17-tetraoxo-5,6,14,15-tetrathia-cyclooctadecaphan-1^4,10^4-diphenyl (**L_2**); 1,11(2,6)-ditriazina-2,10,12,20-tetraaza-3,9,13,19-tetraoxo-6,16-dithia-cyclocosa-phan-1^4,11^4-diphenyl (**L_3**); 1,12(2,6)-ditriazina-2,11,13,22-tetraaza-3,10,14,21-tetraoxo-6,7,17,18-tetrathia-cyclodocosaphan-1^4,12^4-diphenyl (**L_4**) were synthesised. The structural features of the compounds have been studied by elemental analyses, Mass, FT-Raman, FT-IR, ^{1}H and ^{13}C NMR spectroscopy. The antimicrobial activities of the ligands were evaluated using disk diffusion method in dimethyl sulfoxide (DMSO) as well as the minimal inhibitory concentration (MIC) dilution method, against several bacteria and yeast cultures. The obtained results from both methods were assessed in side-by-side comparison with commercial antibacterial and antifungal agents. In most cases, the compounds show strong antifungal activity in the comparison tests. Cytotoxic activities of the ligands against two different human cancer cell lines, stomach (23132/87) and lung (A549) were determined by MTT assay. DNA fragmentation assay tested cell lines were used to analyze the DNA ladder formation which is a characteristic of apoptotic cell death. The binding of the ligands with calf thymus DNA (CT-DNA) has also been investigated by absorption spectroscopy.

1. Introduction

The design and synthesis of macrocyclic compounds having hetero-multi-donor centre have constituted one of the largest areas of research mainly as a result of the roles played by these mixed multi-function materials in: organic and coordination chemistry as ligands, medicinal chemistry as antimicrobials, antitumors and material applications, including dyes and photography [1–7]. Due to structural impact preference, some macrocyclic derivatives play important and fundamental biological functions in nature such as enzymatic actions, photosynthesis, storage and transport of oxygen in mammalian and other respiratory biological systems. In this respect the macrocycles having various donor centres offer exciting possibilities to construct novel supramolecular assemblies that are capable of performing various specific molecular functions [8–11]. For instance, the precise molecular recognition between these ligands and their guests, mostly transition metal ions or biomolecules such as nucleic acids, proteins provide a good opportunity for studying key aspects of supramolecular chemistry, which are also significant in a variety of disciplines including bioorganic chemistry, biocoordination chemistry, biology, medicine and related science and technology [12–17]. Chemically, multi-donor ligands and particularly mixed donor atoms of these ligands are important because of great availability as ligands due to the presence of several potential donor centres and their flexibility to bind with biomolecules or to coordinate with various metal ions. The coordination geometry and properties of most transition metal complexes with numerous hemo and hetero macrocyclic ligands have been studied [18–23]. Among these, the *N–S* donor macrocycles also have theoretical interest, as they are capable of

* Corresponding author. Tel.: +90 212 866 3300; fax: +90 212 866 3402.
E-mail addresses: natabay@fatih.edu.tr, natabay@yahoo.com (N.M. Aghatabay).

0223-5234/$ – see front matter © 2009 Elsevier Masson SAS. All rights reserved.
doi:10.1016/j.ejmech.2009.07.003

furnishing an environment of controlled geometry and ligand field strength such as the Irving–Williams series of stability and hard–soft acid–base principle of Pearson–Parr [24–26].

Metal ions are required for many critical functions in humans. Metal ions can also induce toxicity in humans, classic examples being heavy metal poisons such as mercury, antimony and lead. Toxicity can arise from excessive quantities of either an essential metal, possibly the result of a metabolic deficiency, or a nonessential metal due to contamination or misuse. Detection and detoxification of the toxic metals on humans and as well as environment are one of the most challenging and interesting area of research. Treatment of both as acute and chronic exposure can be studied by chelation therapy [27–31]. Macrocycles having several sulphur donor atoms are critical for soft heavy metal detoxification, because sulphur atoms in its various forms are the primary binding site of many toxic metals [25,26].

The synthesis of these ligands by cycloaddition reactions between amines is well documented [15,32–35]. Recently, attention has been directed towards the use of polydentate aromatic nitrogen heterocycles [36,37]. One possible application of these materials is in generating supramolecular arrays, which embody additional functional groups that are capable of metal complexation. This would result in a metallo-ligand framework with possible potential as novel antimicrobial or therapeutic agents. In this paper, we describe the synthesis and characterization of mixed multidentate macrocycles from 2,4-diamino-6-phenyl-1,3,5-triazine, using 5–8 atom linker dicarboxylic acids. Our principal focus is on the synthesis, spectroscopical characterization and antimicrobial activities due to variation of the macrocycles cavity shape.

2. Experimental protocols

2.1. Chemistry

All chemicals and solvents were reagent grade and were used as purchased without further purification except toluene (Na/benzophenone under N_2). Melting points were determined using an Electro-thermal 9100 melting-point apparatus. Analytical data were obtained with a Thermo Finnigan Flash EA 1112 analyser. UV–vis spectral measurements of the DNA binding studies were carried out on UV-1700 PharmaSpec Shimadzu spectrophotometer. Mass (EI) analyses were carried out in positive ion modes using a Thermo Finnigan LCQ Advantage MAX LC/MS/MS Spectrometer. FT-IR spectra were recorded as KBr pellets on a Jasco FT/IR-600 Plus-Spectrometer. Raman spectra were obtained from powdered samples placed in a Pyrex tube using the Bruker RFS 100/S spectrometer in the range 4000–20 cm^{-1}. The 1064 nm line, provided by a near infrared Nd:YAG air-cooled laser was used as excitation line. The output laser power was set to 180–200 mW. Routine ^1H (400 MHz) and ^{13}C (100 MHz) spectra were recorded at ambient temperature in DMSO-d_6. Chemical shifts (δ) are expressed in units of parts per million relative to TMS. The analytical data, Mass, NMR and physical properties are summarized for each experiment and the prominent vibrational spectral data are presented in Table 1.

2.1.1. Synthesis

*2.1.1.1. 1,9(2,6)-Ditriazina-2,8,10,16-tetraaza-3,7,11,15-tetraoxo-5,13-dithia-cyclohexadecaphan-1⁴,9⁴-diphenyl (**L₁**).* Centrifuged hot ethanolic solution (90 cm^3, absolute) of 2,4-diamino-6-phenyl-1,3,5-triazine (1.25 g, 10 mmol) was mixed with hot ethanolic solution of (10 cm^3) of 2,2-thiodiacetic acid (1.50 g, 10 mmol) in the presence of few drops of concentrated HCl. The solution mixture was refluxed for several hours at 85–90 °C. The white crystalline solid product was formed, which was filtered, washed with cold EtOH and dried under vacuum. The dried solid product was then suspended in dry toluene and the mixture was refluxed using a Dean–Stark trap for 4 h, before the mixture was cooled down, which was then filtered, washed with light petroleum ether and dried under vacuum (1.54 g, 64%). m.p.230 °C. Found (calculated) (**L_1**), [$C_{26}H_{22}N_{10}O_4S_2$]: C, 52.1 (51.8); H, 3.9 (3.7); N, 22.9 (23.3); S, 11.0 (10.6). MS (EI) *m*/*z* (%): 602 (8). ^1H NMR, δ_H 3.37 (s, 8H, CH_2); 6.76 (s, 4H_g); 7.47 (m, 4H_f); 8.25 (d, 2H_h, $J = 7.2$ Hz); 9.0 (br, 4H, NH). $^{13}C\{^1H\}$NMR, δ_C 33.99 (4C, CH_2); 128.15 (4C_f, Ph); 128.58 (4C_g, Ph), 131.51 (2C_h, Ph); 137.49 (2C_e, Ph); 167.86 (4C_c, t-ring); 170.68 (2C_d, t-ring); 171.44 (4C, CO).

The other ligands were prepared in a similar manner to the ligand (**L_1**) and the results are presented as following:

*2.1.1.2. 1,10(2,6)-Ditriazina-2,9,11,18-tetraaza-3,8,12,17-tetraoxo-5,6,14,15-tetrathia-cycloocta-decaphan-1⁴,10⁴-diphenyl (**L₂**).* Hot ethanolic solution (90 cm^3, absolute) of 2,4-diamino-6-phenyl-1,3,5-triazine (1.25 g, 10 mmol) was reacted with ethanolic solution of (10 cm^3) of 2,2-dithiadiacetic acid (1.82 g, 10 mmol) in the presence of few drops of HCl. The white crystalline solid was treated in a Dean–Stark trap (1.80 g, 67%). m.p.197–200 °C. Found (calculated) (**L_2**) 2H_2O, [$C_{26}H_{26}N_{10}O_6S_4$]: C, 44.9 (44.4); H, 3.9 (3.7); N, 20.2 (19.9); S, 17.9 (18.2). MS (EI) *m*/*z* (%): 666 (9), 436 (10), 241(12), 188 (100). ^1H NMR, δ_H 3.68 (s, 8H, CH_2); 6.79 (s, 4H_g); 7.50 (m, 4H_f); 8.26

Table 1
Prominent IR and Raman bands for the (**L_1**–**L_4**) compounds.

Com.	FT-IR (cm^{-1})	Raman (cm^{-1})
(**L_1**)	3371ν(N–H), 3326 ν(N–H), 3178 [ν(CO) + δ(N–H)], 3034 ν(C–H)$_{ar}$, 2980 ν(C–H), 1673 ν(C=O), 1592 ν(C–C)$_{ar}$, 1535 [δ(N–H) + ν(C–N], 1513 ν(C–N)$_{tr}$, 1390, 1361–1273 [ν(C–N) + δ((N–H)], 896, 780 [ω((N–H) + ϕ(C=O)], 687 ω((C–C)$_{ar}$, 621 ν(C–S), 592, 463.	3100, 3069 ν(C–H)$_{ar}$, 2972, 2921 ν(C–H), 1681 ν(C=O), 1601 ν(C–C)$_{ar}$, 1552 ν(C–N)$_{tr}$, 1497 [ν(CO) + δ(N–H)], 1466, 1400, 1181, 1028, 1000, 776 ω((C–H)$_{ar}$, 678, 621 ν(C–S), 95.
(**L_2**)	3467 ν(O–H), 3414 ν(N–H), 3322 [ν(CO) + δ(N–H)], 3127 ν(C–H)$_{ar}$, 2937, 2833 ν(C–H), 1686, ν(C=O), 1648 ν(C–C)$_{ar}$, 1570 [δ(N–H) + ν(C–N], 1530 ν(C–N)$_{tr}$, 1396, 1296–1261 [ν(C–N) + δ((N–H)], 913, 817 [ω((N–H) + ϕ(C=O)], 780 ω((C–C)$_{ar}$, 715, 630 ν(C–S), 586, 470.	3129, 3071 ν(C–H)ar, 2998, 2937 ν(C–H), 1701 ν(C=O), 1651 ν(C=O), 1601 ν(C–C)ar, 1527 [ν(CO) + δ(N–H)], 1504 ν(C–N)$_{tr}$, 1404, 1195, 1156, 1024, 1003, 913, 784 ω((C–H)$_{ar}$, 681, 631 ν(C–S), 573, 505 ν(S–S), 263, 118.
(**L_3**)	3478 ν(O–H), 3440 ν(N–H), 3332, 3215 [ν(CO) + δ(N–H)], 3073 ν(C–H)$_{ar}$, 2975 ν(C–H), 1685 ν(C=O), 1628 ν(C–C)$_{ar}$, 1591 [δ(N–H) + ν(C–N], 1565 ν(C–N)$_{tr}$, 1394–1261 [ν(C–N) + δ((N–H)], 1193, 908, 822 [ω((N–H) + ϕ(C=O)], 785 ω((C–C)$_{ar}$, 709, 621 ν(C–S), 553, 460.	3198, 3081, 3069 ν(C–H)ar, 2936, 2916 ν(C–H), 1646 ν(C=O), 1602 ν(C–C)$_{tr}$, 1538 ν(C–N)$_{tr}$, 1495 [ν(CO) + δ(N–H)], 1399, 1182, 1163, 1004, 781 ω((C–H)$_{ar}$, 676, 616 ν(C–S), 395, 97, 70.
(**L_4**)	3486 ν(O–H), ν(N–H), 3319 [ν(CO) + δ(N–H)], 3123 ν(C–H)$_{ar}$, 2965, 2925 ν(C–H), 1703 ν(C=O), 1673 ν(C=O), 1644 ν(C–C)$_{ar}$, 1568 [δ(N–H) + ν(C–N], 1533 ν(C–N)$_{tr}$, 1399–1203 [ν(C–N) + δ((N–H)], 1062, 820 ω((N–H), 773 ω((C–C)$_{ar}$, 689, 630 ν(C–S).	3064, ν(C–H)$_{ar}$, 2968, 2956, 2927, 2912 ν(C–H), 1708 ν(C=O), 1684 ν(C=O), 1622, 1605 ν(C–C)$_{tr}$, 1578 ν(C–N)$_{tr}$, 1504 [ν(CO) + δ(N–H)], 1404, 1362, 1003, 778 ω((C–H)$_{ar}$, 682, 628 ν(C–S), 612, 601, 568, 508 ν(S–S), 487, 130, 90.

ν, stretching; δ, bending; ω, out-of-plane wagging; ar, aromatic ring; tr, triazine ring.

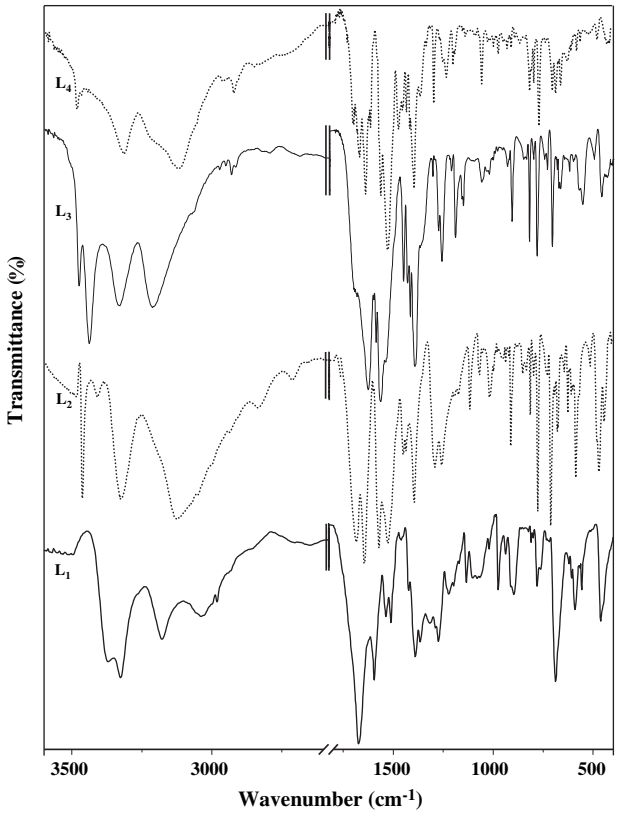

Fig. 1. FT-IR spectrum of ($\mathbf{L_1}$–$\mathbf{L_4}$) ligands in the 3600–2600/1800–400 cm^{-1} regions.

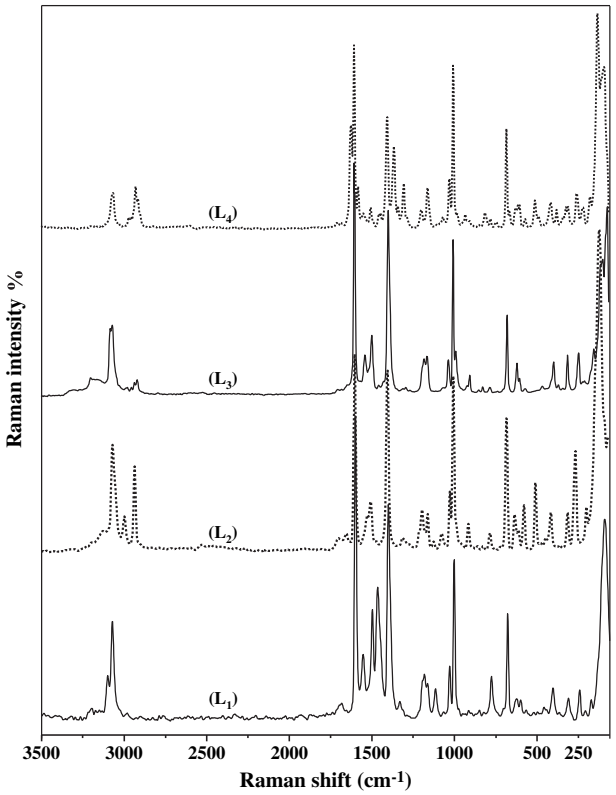

Fig. 2. FT-Raman spectra of ($\mathbf{L_1}$–$\mathbf{L_4}$) in the 3500–60 cm^{-1} region.

(d, $2H_h$, $J = 9.4$ Hz); 9 (br, 4H, NH). $^{13}C\{^1H\}$ NMR, δ_C 41.55 (4C, CH_2); 128.53 ($4C_f$, Ph); 128.99 ($4C_g$, Ph); 131.91 ($2C_h$, Ph); 137.89 ($2C_e$, Ph); 168.26 ($4C_c$, t-ring); 171.04 ($2C_d$, t-ring); 171.41 (4C, CO).

*2.1.1.3. 1,11(2,6)-Ditriazina-2,10,12,20-tetraaza-3,9,13,19-tetraoxo-6,16-dithia-cyclocosa-phan-1^4,11^4-diphenyl (**L$_3$**).* Hot ethanolic solution (90 cm^3, absolute) of 2,4-diamino-6-phenyl-1,3,5-triazine (1.25 g, 10 mmol) was reacted with ethanolic solution of (10 cm^3) of 3,3-thiodipropionic acid (1.78 g, 10 mmol) in the presence of few drops of HCl. The white crystalline solid was treated in a Dean–Stark trap (2.34 g, 82%). m.p. 210 °C. Found (calculated) (**L$_3$**) $(H_2O)_2$, [$C_{30}H_{34}N_{10}O_6S_2$]: C, 51.3 (51.9); H, 5.2 (4.9); N, 2.7 (20.2); S 9.5 (9.2). MS (EI) *m/z* (%): 658 (not detected), 360, 229. ^1H NMR, δ_H 2.51 (t, $J = 6.8$ Hz, 8H, CH_2–CO); 2.70 (t, $J = 6.8$ Hz, 8H, S–CH_2) 6.76 (s, $4H_g$); 7.47 (m, $4H_f$); 8.26 (d, $2H_h$, $J = 7.2$ Hz); 10 (br, 4H, NH). $^{13}C\{^1H\}$ NMR, δ_C 26.41 (4C, S–CH_2); 34.55 (4C, CH_2–CO); 127.66 ($4C_f$, Ph); 128.08 ($4C_g$, Ph); 130.99 ($2C_h$, Ph); 137.04 ($2C_e$, Ph); 167.41 ($4C_c$, t-ring); 170.23 ($2C_d$, t-ring); 173.01 (4C, CO).

*2.1.1.4. 1,12(2,6)-Ditriazina-2,11,13,22-tetraaza-3,10,14,21-tetraoxo-6,7,17,18-tetrathia-cyclo-docosaphan-1^4,12^4-diphenyl (**L$_4$**).* Hot ethanolic solution (90 cm^3, absolute) of 2,4-diamino-6-phenyl-1,3,5-triazine (1.06 g, 8.5 mmol) was reacted with ethanolic solution of (10 cm^3) of 3,-dithiadipropionic acid (1.78 g, 8.5 mmol) in the presence of few drops of HCl. The off white crystalline solid was treated in a Dean–Stark trap (1.77 g, 70%). m.p.165–166 °C. Found (calculated) (**L$_4$**)(H_2O), [$C_{30}H_{32}N_{10}O_5S_4$]: C, 48.7 (48.6); H, 4.7 (4.3); N, 19.3 (18.90); S, 17.5 (17.3). MS (EI) *m/z* (%): 722 (12). ^1H NMR, δ_H 2.64 (t, $J = 6.8$ Hz, 8H, CH_2–CO); 2.91 (t, $J = 6.8$ Hz, 8H, S–CH_2) 6.81 (s, $4H_g$); 7.50 (m, $4H_f$); 8.27 (d, $2H_h$, $J = 9.9$ Hz); 10 (br, 4H, NH). $^{13}C\{^1H\}$ NMR, δ_C 33.51 (4C, S–CH_2); 34.00 (4C, CH_2–CO); 128.17 ($4C_f$, Ph); 128.64 ($4C_g$, Ph); 131.67 ($2C_h$, Ph); 137.17 ($2C_e$, Ph); 167.75 ($4C_c$, t-ring); 170.80 ($2C_d$, t-ring); 173.29 (4C, CO).

2.2. Pharmacology

The antimicrobial activities are evaluated against Gram positive (*Staphylococcus aureus* ATCC 6538, *Bacillus cereus* ATCC 7064, *Mycobacterium smegmatis* CCM 2067, *Listeria monocytogenes* ATCC 15313, *Micrococcus luteus* La 2971) and Gram-negative (*Escherichia coli* ATCC 11230, *Klebsiella pneumoniae* UC57, *Pseudomonas aeruginosa* ATCC 27853, *Proteus vulgaris* ATCC 8427, *Enterobacter aerogenes* ATCC 13048) bacteria and the yeast cultures (*Candida albicans* ATCC 10231, *Kluyveromyces fragilis* NRRL 2415, *Rhodotorula rubra* DSM 70403, *Debaryomyces hansenii* DSM 70238 and *Hanseniaspora guilliermondii* DSM 3432) using both the disk diffusion and the dilution methods.

2.2.1. Methods

2.2.1.1. Disk diffusion. Sterilised antibiotic discs (6 mm) were used following the literature procedure [38,39]. Fresh stock solutions of the ligand and the complex were prepared in DMSO according to the needed concentrations for experiments. To ensure that the solvent had no effect on bacterial growth, a control test was performed with test medium supplemented with DMSO as the same procedures as used in the experiments. All the bacteria were incubated at 30 °C for 24 h in Nutrient Broth. The yeasts were incubated in Malt Extract Broth for 48 h. The discs injected with solutions were placed on the inoculated agar and incubated at 35 °C (24 h) and at 25 °C (72 h) for bacteria and yeast, respectively. On each plate an appropriate reference antibiotic disc was applied depending on the test microorganisms. In each case triplicate tests were performed and the average was taken as the final reading.

2.2.1.2. Dilution. Screening for antibacterial and antifungal activities was carried out by preparing a broth micro dilution, following the procedure outlined in Manual of Clinical Microbial [40]. All the

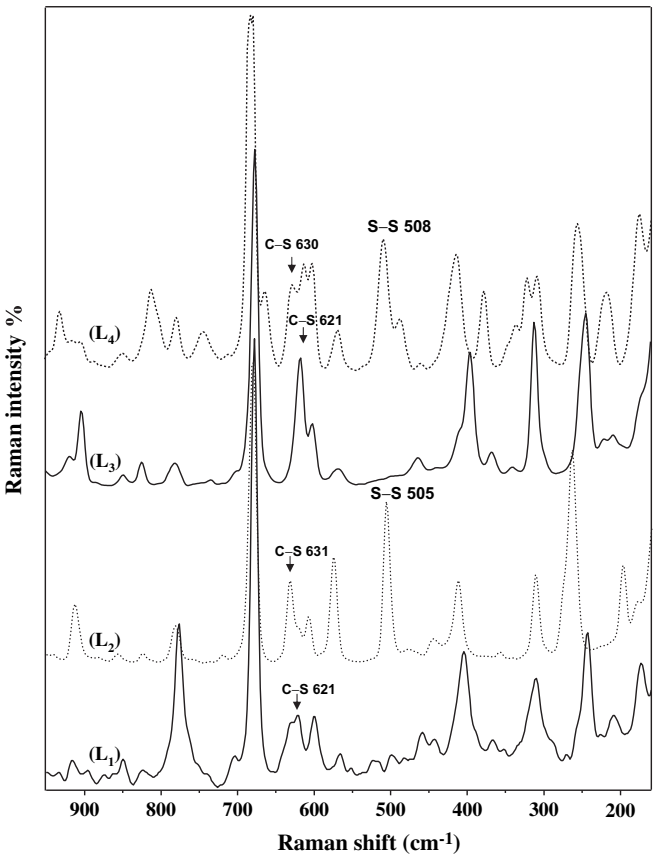

Fig. 3. FT-Raman spectra of ($\mathbf{L_1}$–$\mathbf{L_2}$) compounds in the 950–160 cm^{-1} region.

bacteria were incubated and activate at 30 °C for 24 h inoculation into Nutrient Broth, and the yeasts were incubated in Malt Extract Broth for 48 h. The compounds were dissolved in DMSO (2 mg mL^{-1}) and then diluted using caution adjusted Mueller Hinton Broth (Oxoid). Two-fold serial concentrations of the compounds were employed to determine the (MIC) ranging from 200 μg mL^{-1} to 1.56 μg mL^{-1}. Cultures were grown at 37 °C (20 h) and the final inoculation (inoculums) was approximately 10^6 cfu mL^{-1}. Test cultures were incubated at 37 °C (24 h). The lowest concentrations of antimicrobial agents that result in complete inhibition of microorganisms were represented as (MIC) μg mL^{-1}. In each case triplicate tests were performed and the results are expressed as means.

2.2.1.3. Cytotoxicy. The cytotoxic effect of the ($\mathbf{L_1}$–$\mathbf{L_4}$) ligands against 23132/87 (stomach adenocarcinoma, human) and A549 (non-small cell lung adenocarcinoma, human) were assayed by MTT method [41]. The cells were plated at 37 °C for 24 h on 96-well plates (Grainer) at a density of 3.10^3–5.10^3 cells per well, with RPMI 1640 medium in a humidified atmosphere (5% CO_2). The RPMI 1640 medium was supplemented with 10% (v/v) fetal bovine serum (FBS), 4 mM L-glutamine and antibiotics (penicillin/streptomycin). Freshly prepared ligands (DMSO) were further diluted in complete culture medium and the final volume of DMSO in the culture medium was adjusted to 0.5% (v/v). The seeded cells were exposed to 0.1, 1, 10, 100 μM concentrations of the test compounds for 24 and 48 h at 37 °C in humidified incubator with 5% CO_2 at a final volume of 150 μL. After incubation, 15 μL MTT solutions was added to each well and incubated for further 4 h. The MTT solution then was carefully removed and dissolved by adding 200 μL (DMF 50%, SDS 5%) aqueous solution and analyzed at 570 nm in a microplate reader. Cytotoxicity values were determined using $100\times(OD_{570\text{treated cells}}/OD_{570\text{untreated cell}})$ equation.

2.2.1.4. DNA fragmentation. Tested cell lines were used to analyze the DNA ladder formation which is a characteristic of apoptotic cell death [42]. The cells (10×10^4) were plated on 6 well plates and exposed on the ($\mathbf{L_1}$–$\mathbf{L_4}$) ligands (100 μM) for 24 h. After the incubation the cell lines were collected and washed with PBS (phosphate-buffered saline). The DNA was extracted with the Nucleospin Tissue kit. The extracts were run on 1.5% agarose gel. The products were visualized under UV-light with Bio-Rad Gel Doc gel scanner system.

2.2.1.5. Hoechst 33258 staining [43]. The cells that were cultured on 6 well plates and treated with the compound (100 μM) for 24 h. After the treatment, cells were washed with PBS (3 times) and fixed with ice cold methanol for 10 min. Following fixation, cells were incubated with Hoechst 33258 (5 mg mL^{-1}) for 5 min and then destained with double-distilled water for further 5 min and were examined by fluorescence microscopy (CarlZeis).

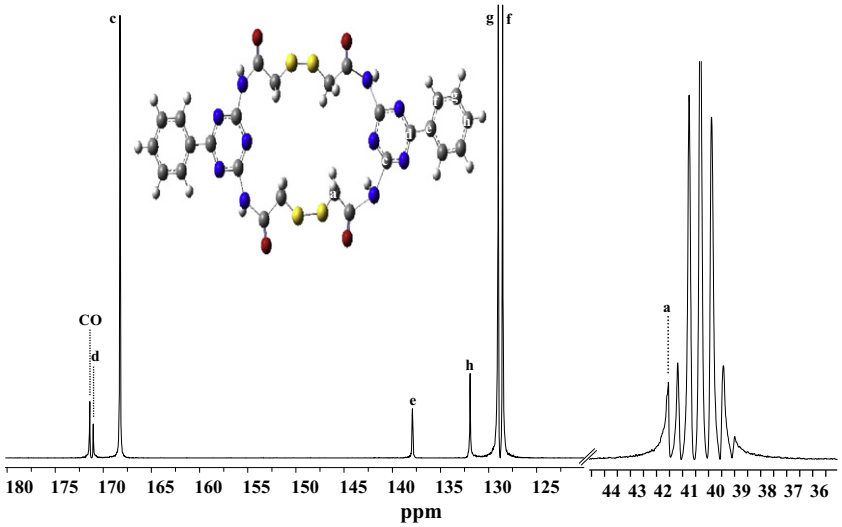

Fig. 4. $^{13}C\{^1H\}$ NMR spectrum of ($\mathbf{L_2}$) ligand.

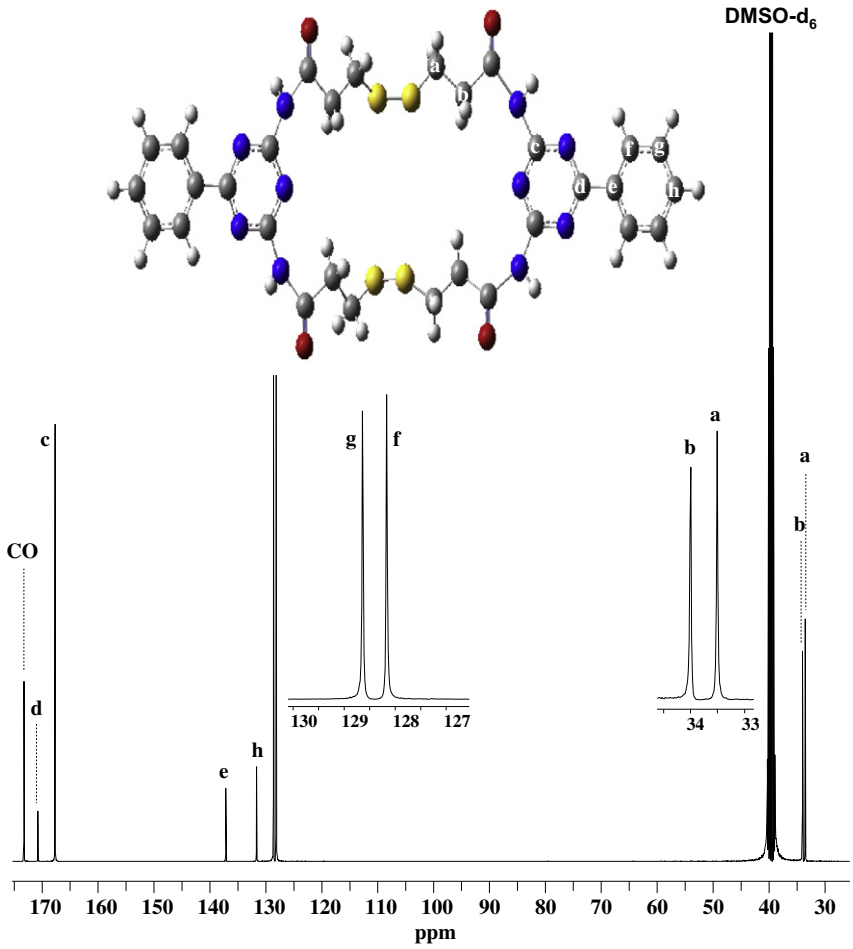

Fig. 5. $^{13}C\{^1H\}$ NMR spectrum of ($\mathbf{L_4}$) ligand.

2.2.1.6. DNA Binding UV–visible. Calf thymus DNA was purchased from Worthington Biochemical Corp. and prepared in ddH_2O at a concentration of 60 μg/μL. Purity of CT-DNA was determined by comparing UV absorbance ratios at 260 and 280 nm (1.8:1), indicating that the DNA was sufficiently free of protein. The absorption spectra of the DNA solution (250 μM) were obtained in the absence and presence of increasing amounts of the ligands [0–500 μM].

2.2.1.7. Biological data. Standardised samples of Penicillin-g blocking the formation of bacterial cell walls, rendering bacteria unable to multiply and spread; Ampicillin (penetrating and preventing the growth of Gram-negative bacteria); Cefotaxime (used against most Gram-negative enteric bacteria); Vancomycin (acting by interfering with the construction cell walls in bacteria), Ofloxacin (entering the bacterial cell and inhibiting DNA-gyrase, which is involved in the production of genetic material, preventing the bacteria from reproducing); Tetracyclines exerting their antimicrobial effect the inhibition of protein synthesis; Nystatin (binding to sterols in the fungal cellular membrane altering the permeability to allow leakage of the cellular contents and destroying the fungus); Ketoconazole (inhibiting the growth of fungal organisms by interfering with the formation of the fungal cell wall) and Clotrimazole (interfering with their cell membranes and causing essential constituents of the fungal cells leakage). Mueller Hinton media, Nutrient Broth and Malt Extract Broth are purchased from Difco and yeast extracts is obtained from Oxoid.

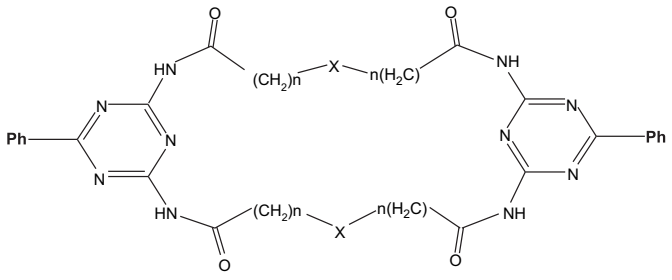

Fig. 6. General proposed structure of the ligands: ($\mathbf{L_1}$), $n = 1$, X = S; ($\mathbf{L_2}$), $n = 1$, X = S–S;($\mathbf{L_3}$), $n = 2$, X = S; ($\mathbf{L_4}$), $n = 2$, X = S–S.

3. Results and discussion

3.1. Vibrational spectra

The present vibrational spectra can be discussed in terms of three characteristic wave regions: 3570–2850 cm^{-1} corresponding to ν(H–O–H) lattice water, ν(N–H) amides and ν(C–H) aliphatic and aromatic characteristic modes, 1800–800 cm^{-1} belongs to ν(CONH–) amides, $\nu(C–N)_{tr}$, δ(N–H) and 750–500 cm^{-1} frequencies regions due to the ν(C–S) and ν(S–S) characteristic stretching modes, which are clearly assignable in the Raman spectra. Prominent Raman and IR frequency data values and their some assignments are presented in Table 1. Appearance of a strong broad band in the region 3490–3380 cm^{-1} in the IR spectra may be due to the presence of lattice water (H–O–H) (antisymmetric and symmetric), which was also confirmed by elemental analysis [44]. These modes are either very

Table 2
In vitro antimicrobial activity of the (**L_1–L_4**) compounds and the standard reagents (inhibition zone mm).

Microorganisms/compounds	(**L_1**)	(**L_2**)	(**L_3**)	(**L_4**)	P10	AMP	CTX	VA	OFX	TE	NY	KET	CLT
Escherichia coli	10.0	10.0	10.0	10.0	18	12	10	22	30	28	–	–	–
Staphylococcus aureus	12.0	14.0	10.0	12.0	13	16	12	13	24	26	–	–	–
Klebsiella pneumoniae	13.0	15.0	13.0	16.0	18	14	13	22	28	30	–	–	–
Bacillus cereus	14.0	17.0	13.0	15.0	8	10	54	10	44	34	–	–	–
Micrococcus luteus	14.0	18.0	12.0	17.0	10	16	18	20	28	26	–	–	–
Proteus vulgaris	12.0	11.0	11.0	13.0	14	12	14	18	30	25	–	–	–
Mycobacterium smegmatis	10.0	10.0	9.0	11.0	15	21	11	20	32	24	–	–	–
Listeria monocytogenes	10.0	10.0	10.0	10.0	10	12	16	26	30	28	–	–	–
Pseudomonas aeruginose	9.0	11.0	11.0	11.0	36	32	32	34	28	22	–	–	–
Kluyveromyces fragilis	15.0	19.0	16.0	21.0	–	–	–	–	–	–	20	21	15
Rhodotorula rubra	17.0	18.0	16.0	21.0	–	–	–	–	–	–	18	16	18
Candida albicans	16.0	19.0	19.0	19.0	–	–	–	–	–	–	18	22	16
Hanseniaspora guilliermondii	20.0	20.0	19.0	22.0	–	–	–	–	–	–	21	24	22
Debaryomyces hansenii	18.0	21.0	18.0	22.0	–	–	–	–	–	–	16	14	18

P10, Penicillin G (10 Units); AMP, Ampicillin 10 μg; CTX, Cefotaxime 30 μg; VA, Vancomycin 30 μg; OFX, Ofloxacin 5 μg; TE, Tetracycline 30 μg; NY, Nystatin 100 μg; KET, Ketoconazole 20 μg; CLT, Clotrimazole 10 μg.

weak or not active in Raman spectra. The bands corresponding to free carboxylic acid (–COOH) and amine ($–NH_2$) groups are not observed in the IR spectra of the (**L_1–L_4**) ligands, which suggests complete condensation of the amine groups of 2,4-diamino-6-phenyl-1,3,5-triazine with corresponding dicarboxylic acids. The bands observed in the regions 3300 and 3150 cm^{-1} in the IR spectra are assignable to amide A and amide B vibration respectively. The amide A is almost caused by the NH stretching vibration, this mode of vibration is not depend on the backbone conformation but is very sensitive to the strength of a hydrogen bonding. The amide B is originates from a Fermi resonance between the first overtone of amide II and the N–H stretching vibration [45,46]. Due to non-planar characteristic behaviour of the compounds in the solid state, the bands could be observed as multiple signals. These lines have extremely weak Raman intensity, particularly in the solid form (Figs. 1 and 2). The pure characteristic ν(CH) modes of aliphatic groups are observed in the wave region 2930–2820 cm^{-1} in both Raman and IR spectra as expected. The peptide bond formation could also be confirmed due to the observance of two major bands in the frequency regions 1700–1650 cm^{-1} (amide I) and 1590–1540 cm^{-1} (amide II). The amide I band is the most intensive absorption band particularly in the IR spectrum and it is almost fully governed by the stretching vibration of the C═O mode with a very small contribution of the C–N groups. Amide II is more complex than amid I, which derives mainly from in-plane N–H bending vibration with certain contribution of ν(C–N) groups. Amide III and IV are very complex bands resulting from a mixture of several coordinate displacements. These modes are dominated by the out-of-plane motions particularly (N–H) wagging and (C═O) deformation vibrations as reported in the Table 1 [45,46]. The bending vibrations for δ(H–O–H) in IR spectra are observed in the region 1640 cm^{-1} (Figs. 1 and 2).

Table 3
.*In vitro* antimicrobial activity (MIC, μg mL^{-1}) of the (**L_1–L_4**) compounds.

Microorganisms/Compounds	(**L_1**)	(**L_2**)	(**L_3**)	(**L_4**)	GEN	NYS
Escherichia coli	25	25	25	25	6.25	–
Staphylococcus aureus	12.5	12.5	25	12.5	25	–
Klebsiella pneumoniae	12.5	6.25	12.5	6.25	6,25	–
Bacillus cereus	6.25	3.125	12.5	6.25	6.25	–
Micrococcus luteus	12.5	3.125	12.5	6.25	25	–
Proteus vulgaris	12.5	25	25	12.5	6.25	–
Mycobacterium smegmatis	25	25	50	25	12.5	–
Listeria monocytogenes	25	25	25	25	12.5	–
Pseudomonas aeruginose	50	25	25	25	6.25	–
Kluyveromyces fragilis	6.25	1.56	6.25	1.56	–	6.25
Rhodotorula rubra	6.25	3.125	6.25	3.125	–	6.25
Candida albicans	6.25	3.125	3.125	3.125	–	3.125
Hanseniaspora guilliermondii	1.56	1.56	1.56	1.56	–	3.125
Debaryomyces hansenii	3.125	1.56	3.125	1.56	–	12.5

GEN, Gentamycin; NYS, Nystatin.

The vibrational frequency of ν(R–S–S–R) (R = Alkyl) is observed in the region 520–480 cm^{-1} [47]. In the Raman spectra, ν(C–S) and ν(S–S) modes for the (C–S–C) and (C–S–S–C) moieties are very characteristic giving rise to a medium to strong stretching bands in the wave region 710–570 and 530–500 cm^{-1}, respectively [47,48]. The medium to strong bands at 508 of (**L_2**) and 505 cm^{-1} of (**L_4**) clearly show characteristic ν(S–S) stretching modes for these macrocycles (Fig. 3). The assignments are supported by the fact that the other relevant bands at this region remain almost unchanged among these compounds. No clear-cut assignments are possible for ν(C–S) modes, but bands at ca. 530–520 cm^{-1} could be assignable for these particular vibrations (Fig. 3). Because of the non-polar character of the (C–S) and (S–S) modes, their counterpart in IR are quite weak (Table 1, Fig. 1).

3.2. Nuclear magnetic resonance

The ^{1}H NMR spectra of the (**L_1–L_4**) ligands in DMSO-d_6 do not give any signal corresponding to primary amine $–NH_2$ (at 6.8 ppm) and carboxylic acid –COOH (ca. 11 ppm), instead they show broad bands in the region 10–9 ppm corresponding to amide (4H) protons. The low field position as well as broadness of NH protons could be attributed to the combination of deshielding via weak hydrogen bonding due to amide and sulphur atoms. As expected no significant changes are observed for the phenyl protons chemical shifts compared with starting material. Two singlets at 3.37 and 3.68 ppm are attributed to the methylene protons of $S–CH_2–CO$ groups for the (**L_1**) and (**L_2**) ligands, respectively. Two triplets are observed for the (**L_3**) and (**L_4**) ligands at 2.70, 2.51 and 2.91, 2.64 ppm for the methylene protons of $S–CH_2–CH_2–CO$ (8H) and $S–S–CH_2–CH_2–CO$ (8H) groups, respectively. Considering the slight stronger deshielding characteristic of sulphur atoms compared with amide groups, the slight higher chemical shift values 2.70 (**L_3**) and 2.91 (**L_4**), may be assignable to the methylene protons that are adjacent to the sulphur atoms [49].

No significant changes are expected for the phenyl and triazine carbon chemical shift values due to the cyclic formation. The phenyl-triazine carbon atom chemical shifts are observed approximately at: 170–171 (C_d), 67–168 (C_c), 137–138 (C_e), 131–132 (C_h), 128–129 (C_g), 128 (C_f) [50]. The signals in the 171–173 ppm regions are assignable to CO of the CO–NH amide group. Similarly two singlets at 33.75 and 40.97 ppm are attributed to methylene carbons of $S–CH_2–CO$ group for (**L_1**) and (**L_2**) ligands, respectively.

Two singlets are appeared for each of the (**L_3**) and (**L_4**) ligands at 26.41, 34.55 and 33.51, 34.0 ppm for methylene carbons of $S–CH_2–$

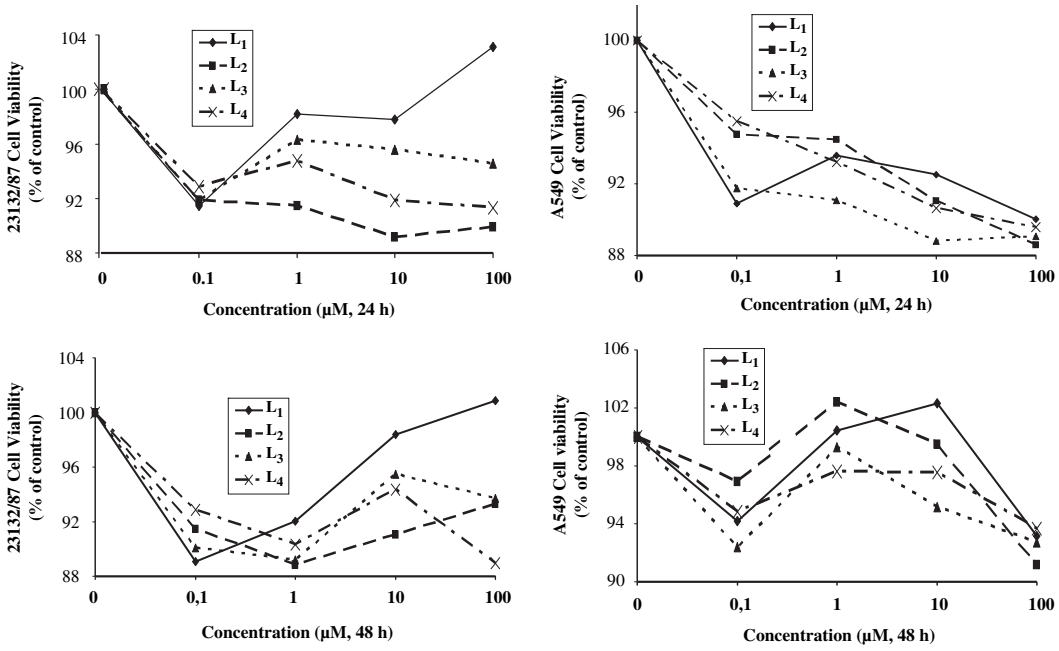

Fig. 7. Effect of the ligands on the viability of 23132/87 and A549 cell lines (0–100 μM, 24, 48 h).

CH_2–CO and S–S–CH_2–CH_2–CO residues, respectively. Considering the weaker deshielding characteristic of sulphur atoms in comparison with amide group on the carbon chemical shift values, the lower ppm values 26.41 (**L_3**) and 33.51 (**L_4**), may be assignable to the methylene carbons that are close to the sulphur atoms (Figs. 4 and 5) [51]. In conclusion, presented generic structure in Fig. 6 is in best accord with the experimental data obtained from the analytical, vibrational and nuclear magnetic resonance spectra.

3.3. Biological activity

3.3.1. Antimicrobial activity

The results concerning in vitro antimicrobial activities of the macrocycles together with the inhibition zone (mm) and (MIC) values of compared antibiotic and antifungal reagents are listed in Tables 2 and 3. All the compounds tested exhibit strong or moderate antimicrobial activity. Of all the test compounds at tempted, (**L_2**) and (**L_4**) showed slightly higher activities against most Gram positive than Gram negative bacteria, but all compounds show strong activity on the yeast cultures. The MIC values in Table 3 indicate that all the compounds tested exhibit moderate to strong antimicrobial activity on the tested microorganisms.

Once again the data indicate that the (**L_2**) and (**L_4**) macrocycles have slightly stronger activity against some Gram positive bacteria such as *Bacillus cereus* (**L_2** = 3.125 and **L_4** = 6.25 μg mL^{-1}) and *Micrococcus luteus* (**L_2** = 3.125 and **L_4** = 6.25 μg mL^{-1}) compared with Gentamycin on these microorganisms 25 and 6.26 μg mL^{-1},

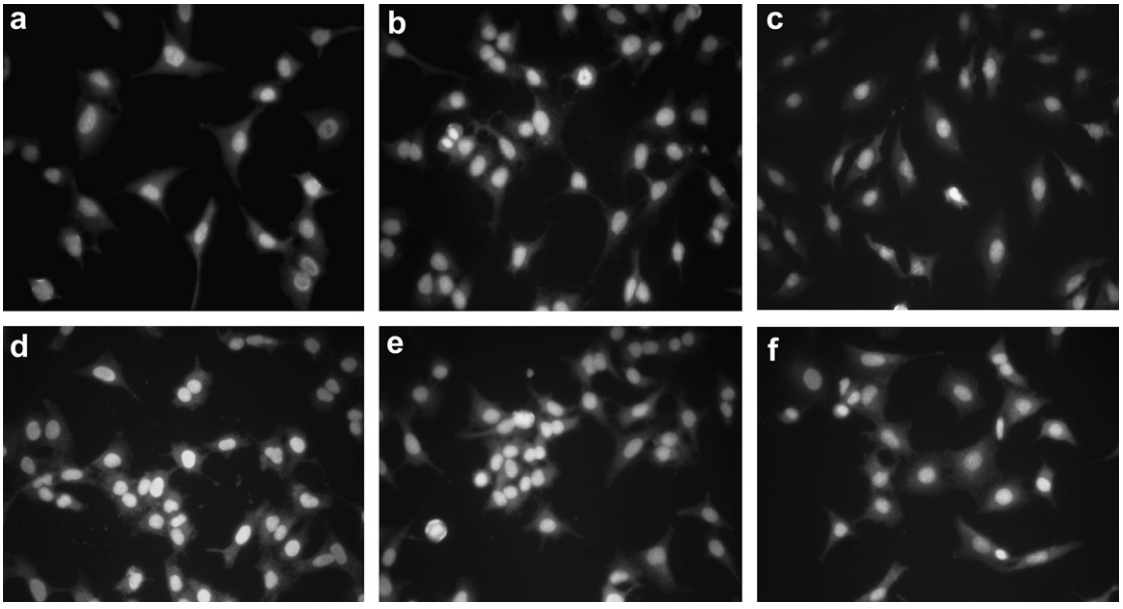

Fig. 8. Hoechst nuclear staining of A549 cells with (100 μM, 24 h) a, untreated; (b–e) with (**L_1**–**L_4**), respectively; f, treated DMSO.

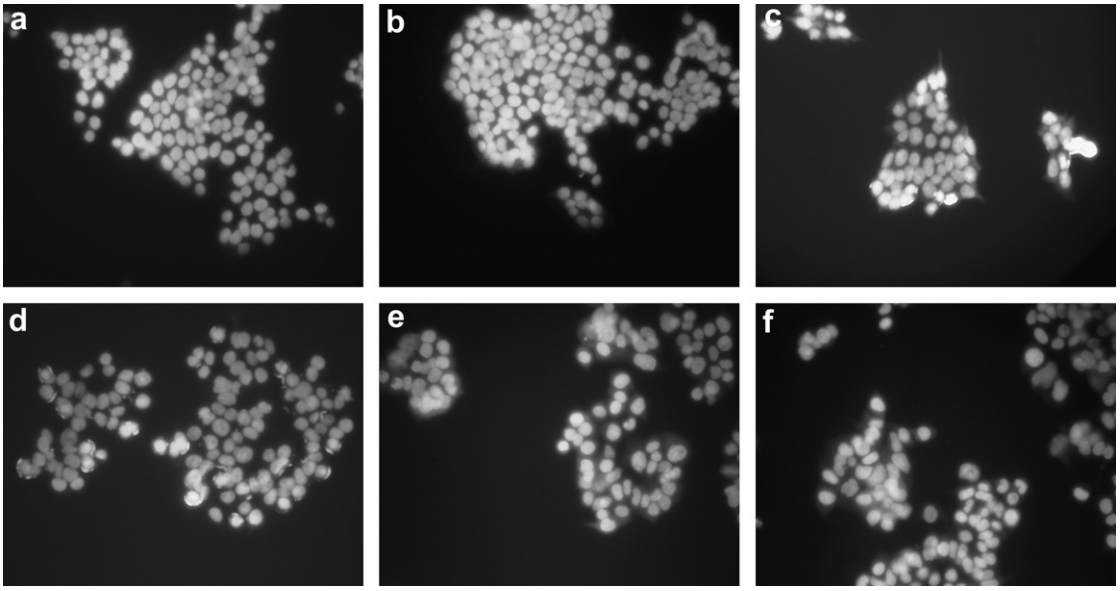

Fig. 9. Hoechst nuclear staining of 23132/87 cells with (100 μM, 24 h) a, untreated; (b–e) with (**L_1–L_4**), respectively; f, treated DMSO.

respectively (Table 3). Similarly these two compounds show same activity with Gentamycin against Gram negative *Klebsiella* bacteria (6.25 μg mL^{-1}). All the tested compounds show very strong activity against the yeast cultures. For instance, all the compounds tested showed superior activity (MIC = 1.56 μg mL^{-1}) against *Hanseniaspora guilliermondii* culture compared with Nystatin antifungal agent. Once more the data indicate that the (**L_2**) and (**L_4**) macrocycles have stronger activity against yeast cultures *Kluyveromyces fragilis* (1.56 μg mL^{-1}) and *Debaryomyces hansenii* (1.56 μg mL^{-1}) in comparison with Nystatin antifungal agent, showing MIC values 6.25 and 12.50 μg mL^{-1} on the same micro-organisms, respectively.

The inhibition activity of the compounds seems to be governed in certain degree by the percentage amount of the sulphur presence in the compounds, because the dithio (**L_2**) and (**L_4**) macrocycles seems indicate more activity against most micro-organisms, compared to the monothio macrocycles. Furthermore, in classifying the antibacterial activity as Gram positive or Gram negative, it would generally be expected that a much greater number would be active against Gram positive than Gram negative bacteria. This conception seems partially true, but in this study, the compounds are relatively active against on both types of the bacteria and as well as strongly active against yeasts, which may indicate a broad-spectrum affect. The results of our study indicate that the compounds have the potential to generate novel antimicrobial properties by displaying moderate to high affinities for most of the receptors particularly against yeast cultures.

3.3.2. Cytotoxicity

The pattern of cytotoxic activity of the ligands is similar to each other and indicates that none of the ligand shows significant cytotoxic effect on the tested cell lines. Cytotoxicity ranges from 0 to 14% for both of the cell lines, indicating a high percentage of the cell lines capability to survive (86–100%). There was a fluctuation in the survival of the cells lines (86–100%) in a dose-independent manner (Fig. 7). In certain cases the survival rates seems increased suggesting an attempt of the cell to develop a defence mechanism

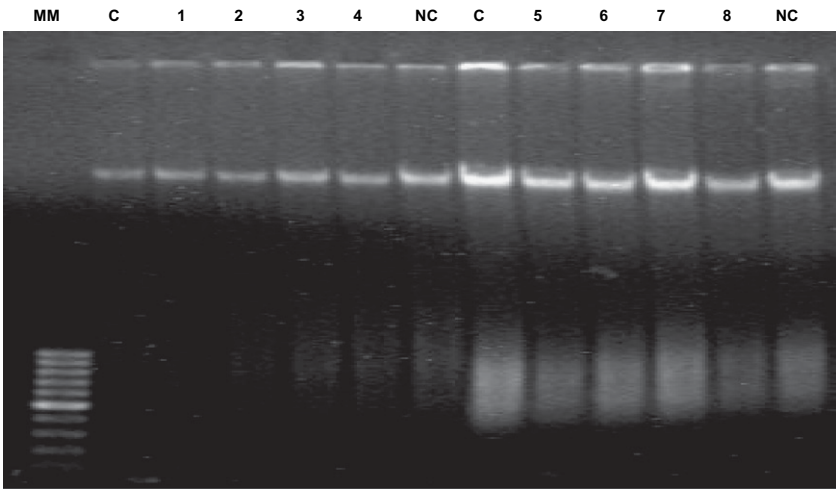

Fig. 10. Gel electrophoresis lines (1–4) 23132/87 cells treated (**L_1–L_4**) (100 μM, 24 h); lines (5–8) A549 cells treated (**L_1–L_4**) (100 μM, 24 h); MM, 100 bp molecular marker; NC, DNA extracted from cells treated with DMSO (24 h); C, untreated cells.

against the ligands. In overall, these compounds seem to have a very low toxic effect against tested cell lines.

3.3.3. Detection of apoptosis

To analyze the effects of the compounds on DNA of the cell lines, we performed nuclear Hoechst staining and DNA fragmentation assays that give clue about the apoptotic cell death. Following Hoechst staining under inverted fluorescence microscope, the nucleus of apoptotic cells can be differentiated from the nucleus of non-apoptotic cells due to DNA damage. We observed that the control and the treated cells had the same nuclear appearance following Hoechst staining (Figs. 8 and 9).

DNA fragmentation which is another indication for apoptosis was tested following treatment of the cell lines with compounds. DNA of the cell lines was intact suggesting that these ligands do not induce DNA fragmentation. The experiment did not indicate any apoptotic cell death and therefore no further experiments were performed (Fig. 10).

3.3.4. DNA binding

Electrostatic or direct hydrogen bonding of the macrocyclic ligands with DNA is expected to bring about marked changes in its electronic spectrum. However, no marked changes have been observed in the electronic spectrum of the DNA with the addition of the ligands, ruling out the possibility of their direct binding to DNA. With the addition of ligands, the DNA systems exhibit only small changes in their electronic spectrum. Such a small change may arise with groove binding, leading to small perturbations. This hyperchromism in the absorption intensity may probably be due to the dissociation of ligand aggregates [52] or due to its external contact (surface binding) with the ligands [53]. Rather small changes in UV–vis spectra did not allow calculation of binding constants (log Ks) for any of the ligands.

Acknowledgement

We would like to extend our gratitude to the Fatih University Scientific Research Centre for their financial support under project-P50020702.

References

[1] T.W. Hambley, L.F. Lindoy, J.R. Reimers, P. Turner, W. Wei, A.N.W. Cooper, J. Chem. Soc., Dalton Trans. (2001) 614.
[2] R.R. Fenton, R. Gauci, P.C. Junk, L.F. Lindoy, R.C. Luckay, G.V. Meehan, J.R. Price, P. Turner, G. Wei, J. Chem. Soc., Dalton Trans. (2002) 2185.
[3] S. Chandra, R. Kumar, Spectrochim. Acta, Part A 61 (2005) 437.
[4] A. Freiria, R. Bastida, L. Valencia, A. Macias, C. Lodeiro, H. Adams, Inorg. Chim. Acta 359 (2006) 2383.
[5] N.M. Agh-atabay, A. Neshat, T. Karabiyik, M. Somer, D. Haciu, B. Dulger, Eur. J. Med. Chem. 42 (2007) 205.
[6] A.D. Bond, A. Fleming, F. Kelleher, J. McGinley, V. Prajapati, S. Skovsgaard, Tetrahedron 63 (2007) 6835.
[7] R.T. Watson, C. Hu, D.G. VanDerveer, D.T. Musashe, P.S. Wagenknecht, Inorg. Chem. Commun. 9 (2006) 180.
[8] B. Blanco, M. Moreno-Manas, R. Pleixats, M. Mehdi, C. Reye, J. Mol. Catal. A Chem. 269 (2007) 204.
[9] N. Kuhnert, D. Marsh, D.C. Nicolau, Tetrahedron: Asymmetry 18 (2007) 1648.
[10] V.E. Semenov, A.D. Voloshina, E.M. Toroptzova, N.V. Kulik, V.V. Zobov, R.K. Giniyatullin, A.S. Mikhailov, A.E. Nikolaev, V.D. Akamsin, V.S. Reznik, Eur. J. Med. Chem. 41 (2006) 1093.
[11] P. Rajakumar, M.G. Swaroop, S. Jayavelu, K. Murugesan, Tetrahedron 62 (2006) 12041.
[12] N.M. Aghatabay, M. Mahmiani, H. Çevik, B. Dulger, Eur. J. Med. Chem. (2008). doi:10.1016/j.ejmech.
[13] F. Marques, L. Gano, M.P. Campello, S. Lacerda, I. Santos, L.M.P. Lima, J. Costa, P. Antunes, R. Delgado, J. Inorg. Biochem. 100 (2006) 270.
[14] M. Tabata, A.K. Sarker, E. Nyarko, J. Inorg. Biochem. 94 (2003) 50.
[15] S. Chandra, L.K. Gupta, Spectrochim. Acta, Part A 60 (2004) 1563.
[16] M.M.A. Boojar, A. Shockravi, Bioorg. Med. Chem. 15 (2007) 3437.
[17] Y. Liu, Tetrahedron Lett. 48 (2007) 3871.
[18] M. Salavati-Niasari, F. Davar, Polyhedron 25 (2006) 2127.
[19] M. Salavati-Niasari, F. Davar, Inorg. Chem. Commun. 9 (2006) 175.
[20] J.D. Chartres, N.S. Davies, L.F. Lindoy, G.V. Meehan, G. Wei, Inorg. Chem. Commun. 9 (2006) 751.
[21] J. Seo, M.R. Song, K.F. Sultana, H.J. Kim, J. Kim, S.S. Lee, J. Mol. Struct. 827 (2007) 201.
[22] S. Chandra, L.K. Gupta, Spectrochim. Acta A 61 (2005) 1181.
[23] H. Khanmohammadi, S. Amani, H. Lang, T. Rüeffer, Inorg. Chim. Acta 360 (2007) 579.
[24] H. Irving, P.J.R. Williams, J. Am. Chem. Soc. (1953) 3192.
[25] R.G. Pearson, J. Am. Chem. Soc. 85 (1963) 3353.
[26] R.G. Parr, R.G. Pearson, J. Am. Chem. Soc. 105 (1983) 751.
[27] J. Aaseth, D. Jacobsen, O. Anderson, E. Wickstrom, Analyst 120 (1995) 853.
[28] M.D. Aleo, M.L. Taub, P.J. Kostyniak, Toxicol. Appl. Pharmacol. 112 (1992) 310.
[29] T. Endo, M. Sakata, Pharmacol. Toxicol. 76 (1995) 190.
[30] J.P.K. Rooney, Rev. Toxicol. 234 (2007) 145.
[31] M. Vahter, Toxicol. Lett. 169 (2007) 91.
[32] P. Rajakumar, A.M.A. Rasheed, A.I. Rabia, D. Chamundeeswari, Bioorg. Med. Chem. Lett. 16 (2006) 6019.
[33] A.S. Girgis, Eur. J. Med. Chem. 43 (2008) 2116.
[34] A.A. Mohamed, G.S. Masaret, A.H.M. Elwahy, Tetrahedron 63 (2007) 4000.
[35] O.V. Kulikof, V.I. Pavlovsky, S.A. Andronati, Chem. Heterocycl. Comp. 41 (2005) 1447.
[36] P. Rajakumar, K. Sekar, V. Shanmugaiah, N. Mathivanan, Eur. J. Med. Chem. 44 (2009) 3040.
[37] D.S. Pilch, C.M. Barbieri, S.G. Rzuczek, E.J. La Voie, J.E. Rice, Biochmie 90 (2008) 1233.
[38] Performance Standards for Antimicrobial Disk Susceptibility Tests, Approved Standard NCCLS Publication M2-A5, Villanova, PA, USA, 1993, pp. 1–32.
[39] C.H. Collins, P.M. Lyre, J.M. Grange, Microbiological Methods, sixth ed. Butterworth Co. Ltd, London, 1989.
[40] R.N. Jones, A.L. Barry, T.L. Gaven, J.A. Washington, Manual of Clinical Microbiology, in: E.H. Lennette, A. Balows, W.J. Shadomy (Eds.), fourth ed. American Society for Microbiology, Washington, DC, 1984, pp. 972–977.
[41] T. Mosmann, J. Immunol. Methods 65 (1983) 55.
[42] S. Kotamraju, C.L. Williams, B. Kalyanaraman, Cancer Res. 67 (2007) 8973.
[43] M.B. Irmak, G. Ince, M. Ozturk, R.C. Atalay, Cancer Res. 63 (2003) 6707.
[44] K. Nakamoto, Infrared and Raman Spectra of Inorganic and Coordination Compounds Part B (1997) pp. 12, 54–55.
[45] H. Günzer, H.-U. Gremlich, IR Spectroscopy an Introduction, Wiley-VCH Verlag GmbH, 69469 Weinheim, Germany, 2002, pp. 224–226.
[46] S. Chandr5fa, L.K. Gupta, Spectrochim. Acta, Part A 62 (2005) 1102.
[47] J. Weidlein, U. Muller, K. Dehnicke, Schwingungsfrequenzen I Hauptgruppenelemente, Germany, 1981 p. 146.
[48] J.B. Lambert, H.F. Shurvell, D.A. Lightner, R.G. Cooks, Organic Structural Spectroscopy, Prentice-Hall, Inc., 1998, pp. 198–199.
[49] W. Kemp, Nmr In Cheistry, A Multinuclear Introduction (1986) pp. 211.
[50] Spectra Databases for Organic Compounds-SDBS (aist.go.jp).
[51] W. Kemp, Nmr In Cheistry, A Multinuclear Introduction (1986) pp. 221.
[52] R. Vijayalakshmi, M. Kanthimathi, V. Subramanian, B. Unni Nai, Biochim. Biophys. Acta 1475 (2000) 157.
[53] R. Tamilarasan, D.R. McMillin, Inorg. Chem. 29 (1990) 2798.